Published March 30, 2015

T cell lipid peroxidation induces ferroptosis and prevents immunity to infection

Mai Matsushita,[1] Stefan Freigang,[1] Christoph Schneider,[1] Marcus Conrad,[2] Georg W. Bornkamm,[3] and Manfred Kopf[1]

[1]Molecular Biomedicine, Institute of Molecular Health Science, Department of Biology, ETH Zurich, 8093 Zurich, Switzerland
[2]Helmholtz Zentrum München, Institute of Developmental Genetics, 85764 Neuherberg, Germany
[3]Helmholtz Zentrum München, Institute of Clinical Molecular Biology and Tumor Genetics, 81377 Munich, Germany

The selenoenzyme glutathione peroxidase 4 (Gpx4) is a major scavenger of phospholipid hydroperoxides. Although Gpx4 represents a key component of the reactive oxygen species–scavenging network, its relevance in the immune system is yet to be defined. Here, we investigated the importance of Gpx4 for physiological T cell responses by using T cell–specific Gpx4-deficient mice. Our results revealed that, despite normal thymic T cell development, $CD8^+$ T cells from $T^{\Delta Gpx4/\Delta Gpx4}$ mice had an intrinsic defect in maintaining homeostatic balance in the periphery. Moreover, both antigen-specific $CD8^+$ and $CD4^+$ T cells lacking Gpx4 failed to expand and to protect from acute lymphocytic choriomeningitis virus and *Leishmania major* parasite infections, which were rescued with diet supplementation of high dosage of vitamin E. Notably, depletion of the Gpx4 gene in the memory phase of viral infection did not affect T cell recall responses upon secondary infection. Ex vivo, Gpx4-deficient T cells rapidly accumulated membrane lipid peroxides and concomitantly underwent cell death driven by ferroptosis but not necroptosis. These studies unveil an essential role of Gpx4 for T cell immunity.

CORRESPONDENCE
Manfred Kopf:
Manfred.Kopf@ethz.ch

Abbreviations used: AIF, apoptosis-inducing factor; aToc, α-tocopherol; DFO, deferoxamine; DN, double negative; DP, double positive; Fer-1, ferrostatin-1; Gpx, glutathione peroxidase; LCMV, lymphocytic choriomeningitis virus; Lm-gp33, *L. monocytogenes* expressing the LCMV gp33 epitope; Nec-1, necrostatin-1; Nec-1i, necrostatin-1 inactive control; RIP, receptor-interacting protein; ROS, reactive oxygen species; SP, single positive; T reg cell, T regulatory cell; $VitE^{hi}$, excess vitamin E; $VitE^{lo}$, low vitamin E.

The balance between production and consumption of reactive oxygen species (ROS) is an important factor in the development and maintenance of multicellular organisms. Cellular ROS are generated endogenously, and the two main sources of intracellular ROS include the family of NADPH oxidases and the mitochondrial respiratory chain, involving complexes I–III (D'Autréaux and Toledano, 2007; Winterbourn, 2008). ROS are critically required for phagocyte-mediated host defense against bacterial and fungal infection (Leto and Geiszt, 2006). Concurrently, it is well appreciated that ROS are at the interface of several cell signaling pathways that regulate cell proliferation, differentiation, and death (D'Autréaux and Toledano, 2007; Finkel, 2011; Ray et al., 2012). Recently, T cell activation, expansion, and effector function have been shown to involve ROS as an important signaling molecule (Wang and Green, 2012; Pearce and Pearce, 2013; Sena et al., 2013). However, ROS can also have detrimental impacts on the organism, and therefore ROS is constantly scavenged to maintain a healthy redox balance under homeostatic control. Disruption of this redox equilibrium leads to increased ROS levels, which can threaten the integrity of various biomolecules including DNA, proteins, lipoproteins and lipids, thereby causing aberrant cell death and tissue deterioration (Marnett, 2002). Indeed, oxidative stress has been implicated in aging (Lambert et al., 2007) and development of a variety of diseases, including cancer (Toyokuni et al., 1995), type 2 diabetes (Brownlee, 2001), atherosclerosis (Galkina and Ley, 2009), and neurodegeneration (Lin and Beal, 2006).

To protect cells and organisms from the detrimental effects caused by excessive ROS formation, aerobic organisms use a network of antioxidant enzymatic pathways. One of the eight members of the glutathione peroxidase (Gpx) family, Gpx4, has been reported as a unique antioxidant enzyme for its ability to directly reduce phospholipid hydroperoxides and oxidized lipoproteins to their respective lipid-alcohol within biomembranes (Thomas et al., 1990; Sattler et al., 1994). Gpx4 functions as a repressor of

The Rockefeller University Press $30.00
J. Exp. Med. 2015 Vol. 212 No. 4 555–568
www.jem.org/cgi/doi/10.1084/jem.20140857

Published March 30, 2015

12/15-lipoxygenase–induced lipid peroxidation that triggers apoptosis-inducing-factor (AIF)–mediated cell death in fibroblasts in vitro (Seiler et al., 2008). The central importance for cellular physiology and normal development of the cytosolic form is highlighted by the embryonic lethality observed in mice with a homozygous Gpx4 deletion (Yant et al., 2003). Also, studies have suggested a synergistic relationship between selenium and vitamin E to inhibit lipid peroxidation (Navarro et al., 1998; Beck et al., 2003).

Despite the importance of Gpx4 as a key component in the ROS scavenging network, its role in the immune system has not been addressed. Here, we have analyzed the physiological relevance of Gpx4 in T lymphocytes by examining the consequences of *Gpx4*-deficiency during thymic development, peripheral T cell homeostasis, and T cell responses to infections with LCMV and *Leishmania major* using *Cd4*-cre/*Gpx4*$^{fl/fl}$ ($T^{\Delta Gpx4/\Delta Gpx4}$) mice. We report that Gpx4 is vital for the homeostatic survival of $CD8^+$ T cells and for the expansion of both $CD4^+$ and $CD8^+$ T cells upon TCR triggering in response to infection by preventing membrane lipid peroxidation and ferroptosis.

RESULTS

Gpx4 promotes maintenance of peripheral $CD8^+$ T cells

To investigate the function of Gpx4 in T cell–meditated immunity and to circumvent the embryonic lethality of global *Gpx4* deficiency, we generated T cell–specific *Gpx4* knockout mice ($T^{\Delta Gpx4/\Delta Gpx4}$) by crossing mice expressing Cre recombinase from the *Cd4* promoter to delete the *lox*P-flanked *Gpx4* alleles specifically at the $CD4^+CD8^+$ double positive (DP) stage of thymic T cell development. Cre-mediated deletion in mature thymocytes and peripheral T cells from $T^{\Delta Gpx4/\Delta GPx4}$ was complete at the mRNA, genomic DNA, and protein levels (Fig. 1, A–D). Development of $CD4^-CD8^-$ double-negative (DN), DP, $CD4^+$ single-positive (SP), and $CD8^+$ SP T cell subsets were intact in $T^{\Delta Gpx4/\Delta Gpx4}$ thymocytes as compared with WT littermate control mice (Fig. 1 E).

Contrary to the thymus, $T^{\Delta Gpx4/\Delta Gpx4}$ mice exhibited considerably fewer $CD8^+$ T cells in the spleen, peripheral LNs, and mesenteric LNs (Fig. 1 F). The defect was nonprogressive, as peripheral $CD8^+$ T cells had equal reduction ratios at 6 and 20 wk of age (Fig. 1 G). Gpx4 deficiency did not affect the homeostasis of T regulatory cells (T reg cells) expressing the transcription factor Foxp3 (Fig. 1 H), and had no difference in activated or memory phenotypes of peripheral $CD4^+$ and $CD8^+$ T cells recognized by CD62L and CD44 cell surface expressions (Fig. 1 I). Importantly, no differences in T cell homeostasis or responses to viral infection (see below) were seen between Gpx4 heterozygous ($T^{\Delta Gpx4/+}$), congenic Cd4-cre, and C57BL/6 mice.

To explore T cell development in a setting where KO T cells compete with WT, we reconstituted irradiated C57BL/6 ($CD45.1^+CD45.2^+$) with an equal ratio of congenically marked donor $T^{\Delta Gpx4/\Delta Gpx4}$ ($CD45.2^+$) and WT ($CD45.1^+$) BM cells. The ratios of $CD45.1^+$ and $CD45.2^+$ T cells were normalized to $B220^+$ BM cells, which served as an internal control to obviate the altered homeostasis that developed in $T^{\Delta Gpx4/\Delta GPx4}$ mice. No differences were observed comparing frequencies of DP and mature SP thymocytes with and without an intact *Gpx4*-gene (Fig. 2 A). In contrast, frequencies of both Gpx4-deficient $CD4^+$ and $CD8^+$ T cells in the spleen were severely compromised (Fig. 2 B). To further address a possible defect in thymocyte expansion that occurs in the DN3/DN4 stage before CD4 expression (and in this case Cre activity), we generated *Gpx4*$^{fl/fl}$ mice expressing the tamoxifen-inducible Cre recombinase construct *Ert2*-Cre downstream of *Rosa-26* promoter (*Rosa26-Ert2-Cre/Gpx4*$^{fl/fl}$ mice, hereafter termed $tam^{\Delta Gpx4/\Delta Gpx4}$ mice). Mixed BM chimeras were generated by reconstituting irradiated C57BL/6 ($CD45.1^+$) mice with 1:1 mixture of WT ($CD45.1^+$) and $tam^{\Delta Gpx4/\Delta Gpx4}$ ($CD45.2^+$) BM cells harvested from mice that were pretreated with tamoxifen 3 d before adoptive transfer. Populations of $tam^{\Delta Gpx4/\Delta Gpx4}$ donor cells in the reconstituted chimeras were maintained in DN, DP, CD4 SP, and CD8 SP T cells, like those derived from WT donor BM (Fig. 2 C). In contrast, numbers of peripheral $CD4^+$ and $CD8^+$ T cells lacking Gpx4 were reduced (Fig. 2 D), as were those in WT/$T^{\Delta Gpx4/\Delta GPx4}$ mixed BM chimeras (Fig. 2 B), confirming that tamoxifen-treatment deleted the *Gpx4* gene in BM hematopoietic precursors cells of $tam^{\Delta Gpx4/\Delta Gpx4}$ mice. These data demonstrate that Gpx4 is dispensable for thymic development and maturation.

We next evaluated lymphopenia-driven expansion of Gpx4-deficient T cells in vivo by adoptively transferring a mixture of equal numbers of $T^{\Delta Gpx4/\Delta Gpx4}$ $CD45.2^+$ and WT $CD45.1^+$ thymocytes into *Rag1*-deficient hosts. In contrast to WT donor cells, which expanded and were maintained after transfer, *Gpx4*-deficient $CD4^+$ and $CD8^+$ T cells were rapidly lost and were nearly undetectable 7 d after transfer (Fig. 2 D). As these results together demonstrate a cell-intrinsic role of Gpx4 for the survival of proliferating $CD4^+$ and $CD8^+$ T cells, we next tested the survival capacity of T reg cells in the absence of Gpx4. Interestingly, IL-2 immune complex–induced expansion of T reg cells was unaffected in $T^{\Delta Gpx4/\Delta Gpx4}$ mice compared with controls (Fig. 2 E). These results highlight that the requirement of Gpx4 for survival differs among T cell subsets.

Gpx4 is critical for T cell expansion and protection from viral and parasitic infection

We next examined the impact of Gpx4 on T cell expansion driven by acute infection with lymphocytic choriomeningitis virus (LCMV)-WE (200 pfu). We found significantly fewer splenic $CD4^+$ and $CD8^+$ T cells in $T^{\Delta Gpx4/\Delta Gpx4}$ compared with WT mice (Fig. 3 A). Moreover, virus-specific $CD8^+$ and $CD4^+$ T cells were undetectable in the spleen of $T^{\Delta Gpx4/\Delta Gpx4}$ mice by MHC class I and class II tetramers loaded with LCMV gp_{33-41} and gp_{61-80} peptides, respectively, indicating that Gpx4-deficient T cells failed to expand (Fig. 3, B and C). Furthermore, to avoid potential secondary effects caused by permanent *Cd4*-cre–mediated Gpx4 deletion, we generated mixed BM chimeras by reconstituting C57BL/6 ($CD45.1^+$) mice with 1:1 mixture of WT ($CD45.1^+$) or $tam^{\Delta Gpx4/\Delta Gpx4}$ ($CD45.2^+$)

Published March 30, 2015

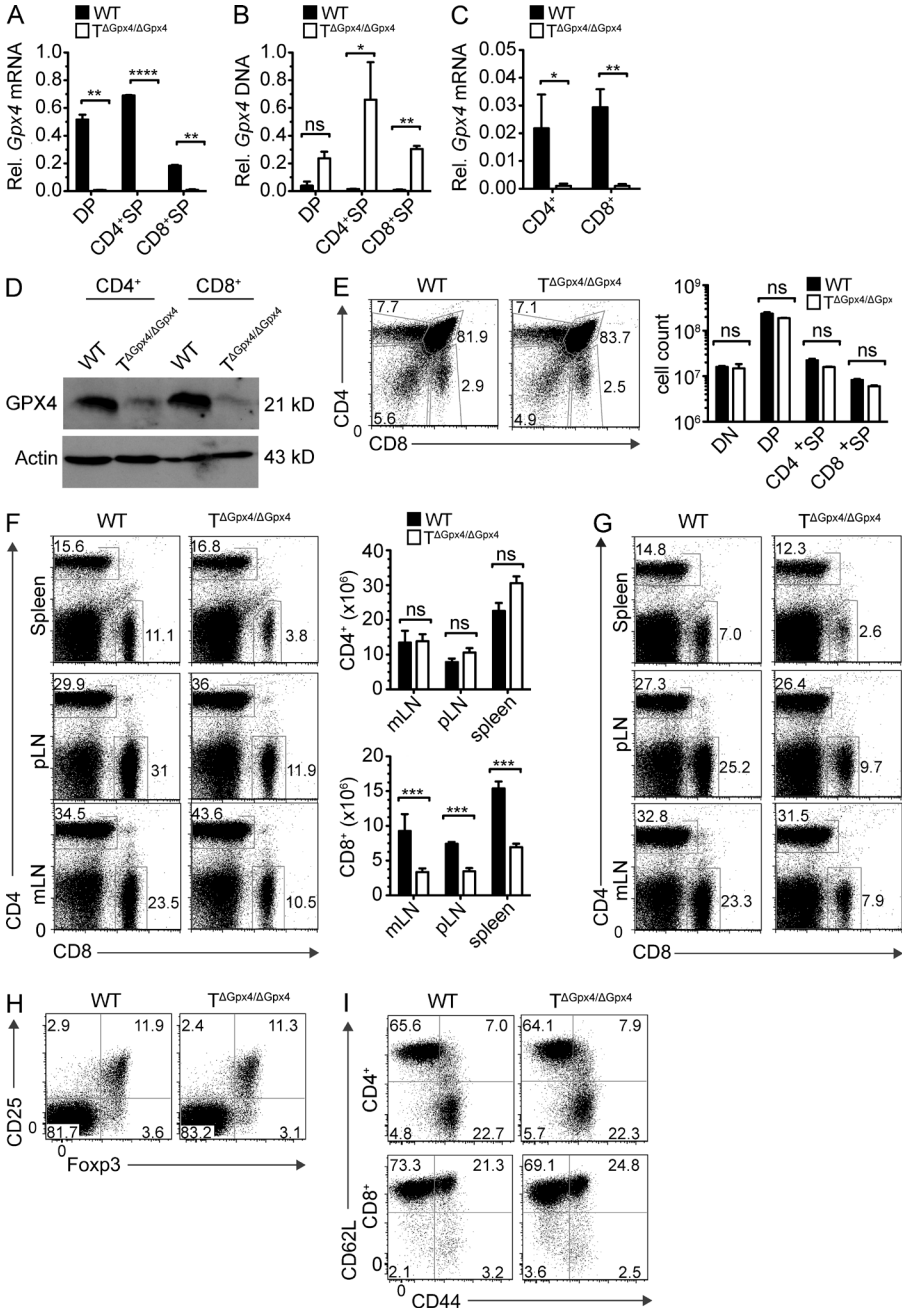

Figure 1. T specific deletion of Gpx4 leads to normal thymocyte development but defective CD8+ T cell homeostasis in the periphery. (A) Analysis of *Gpx4* mRNA in DP, CD4+ SP, or CD8+ SP thymocytes. Results were normalized to *G6pdx* mRNA. (B) Analysis of genomic *Gpx4* DNA in DP, CD4+ SP, or CD8+ SP thymocytes of WT and $T^{\Delta Gpx4/\Delta Gpx4}$ mice to determine the presence of the loxP-flanked neomycin resistance gene. *Gapdh* was used as the housekeeping gene. (C) Real-time PCR analysis of *Gpx4* mRNA in peripheral CD4+ or CD8+ splenocytes. Results were normalized to *G6pdx* mRNA. (D) Western blot of GPX4 expression levels in peripheral CD4+ or CD8+ T cells. Actin was used as a loading control. (E) Representative FACS analysis (left) and absolute number (right) of thymocytes in WT littermate control and $T^{\Delta Gpx4/\Delta Gpx4}$ mice. There are no statistically significant differences in the absolute number of CD4−CD8− double negative (DN), CD4+CD8+ DP, CD4+ SP, or CD8+ SP thymocytes ($n = 4$ mice per group of 6-wk-old mice). (F and G) Flow cytometry analysis of spleen, peripheral LN (pLN), and mesenteric LN (mLN) cells from 6-wk-old (F) and 20-wk-old (G) WT and $T^{\Delta Gpx4/\Delta Gpx4}$ mice (left), and absolute numbers (F, right) of CD4+ (top) or CD8+ (bottom) T cells in the spleen ($n = 4$–5 per group). (H) Analysis of CD4+CD25+Foxp3+ T regulatory cells (T reg cells) in the spleens of WT and $T^{\Delta Gpx4/\Delta Gpx4}$ mice (representative plot from $n \leq 4$ per group). Flow cytometry plots are pregated on CD4+ subsets. (I) Expression of CD62L and CD44 on WT and $T^{\Delta Gpx4/\Delta Gpx4}$ mice splenic T cells. Plots are pregated on CD4+ (top) or CD8+ (bottom; representative plot from $n = 3$ per group of 6-wk-old mice). *, $P \leq 0.05$; **, $P \leq 0.01$; ***, $P \leq 0.001$; ****, $P \leq 0.0001$; ns, not significant (two-tailed Student's *t* test). Data are representative of four independent experiments.

BM cells and WT (CD45.1+) BM cells, and infected the chimeras with LCMV-WE. In accordance with the findings from $T^{\Delta Gpx4/\Delta Gpx4}$ mice, tamoxifen-induced deletion of Gpx4 before infection also resulted in a significant decrease in total CD4+, CD8+, and gp_{33-41}+ T cells (Fig. 3 D). Accordingly, $T^{\Delta Gpx4/\Delta Gpx4}$ mice failed to clear the virus from the blood (Fig. 3 E) and nonlymphoid organs (i.e., liver, kidney, and lung; Fig. 3 F). To monitor early CD8+ T cell expansion after LCMV infection, we adoptively transferred congenically marked P14 (CD45.1+) and $P14^{\Delta Gpx4/\Delta Gpx4}$ (CD45.2+) transgenic CD8+ T cells, specific for the LCMV gp33 epitope presented on H-2D^b, at equal ratios (1:1) into naive WT recipients (CD45.1+CD45.2+), followed by infection of host mice 2 h after transfer with LCMV-WE. At day 4 after infection, the number of Vα2+CD8+ T cells from $P14^{\Delta Gpx4/\Delta Gpx4}$ were incomparably lower than that of P14 WT cells (Fig. 3 G), suggesting that Gpx4-deficient T cells immediately collapsed after infection. Gpx4 was not only critical for antiviral CD8+ T cell responses, but also for Th1-mediated antiparasitic responses. $T^{\Delta Gpx4/\Delta Gpx4}$ mice infected subcutaneously with *L. major* displayed significant reduction in CD4+ T cells (Fig. 3 H) and persistent parasite load was detected in the footpad, draining LNs, and spleen (Fig. 3 I). These findings demonstrated that Gpx4 is vital for T cell–mediated immunity in vivo.

Published March 30, 2015

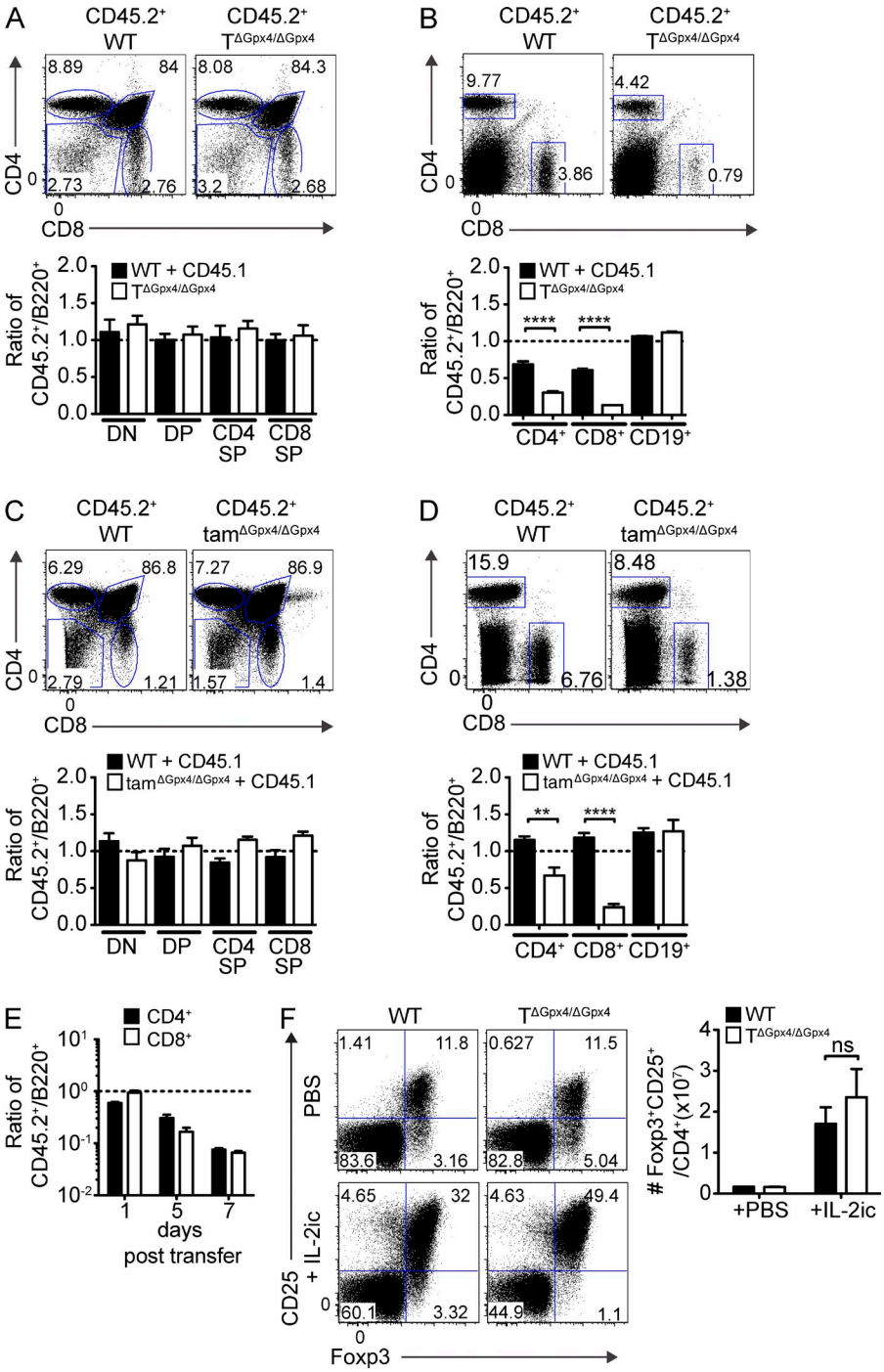

Figure 2. Both CD4+ and CD8+ T cells require Gpx4 for survival and sterile expansion upon transfer into lymphopenic mice. (A and B) Mixed BM chimeras were generated by transfer of a mixture (1:1) of BM stem cells from WT (CD45.1+) or $T^{\Delta Gpx4/\Delta Gpx4}$ (CD45.2+) mice into sublethally irradiated WT (CD45.1+CD45.2+) mice, followed by analysis at 7 wk after reconstitution. Percentages of reconstituted T cell subsets in the thymuses (A) and spleens (B) from WT and $T^{\Delta Gpx4/\Delta Gpx4}$ donors were normalized to B220+ BM frequencies ($n \geq 6$ per group). ****, $P \leq 0.0001$ (Student's *t* test). (C and D) Flow cytometry (top) and ratio (bottom) of thymocytes (C) and splenocytes (D) from mixed BM chimeras generated by transfer of a mixture (1:1) of tamoxifen-treated BM stem cells from WT (CD45.1+) or $tam^{\Delta Gpx4/\Delta Gpx4}$ (CD45.2+) mice into sublethally irradiated WT (CD45.1+) mice. Analysis at 8 wk after reconstitution ($n = 4$ per group). **, $P \leq 0.01$; ****, $P \leq 0.0001$ (Student's *t* test). (E) Ratios of surviving CD4+ and CD8+ T cells in the peripheral blood on days 1, 5 and 7 after adoptive transfer of equal numbers of WT (CD45.1+) and $T^{\Delta Gpx4/\Delta Gpx4}$ (CD45.2+) donor thymocytes into *Rag*-1-deficient mice ($n \geq 6$ per group). (F) Flow cytometry (left) and absolute numbers (right) of splenic T reg cells at 5 d after in vivo expansion of T reg cells by intraperitoneal injection with PBS or interleukin-2 (IL-2) and anti-IL-2 antibody complex into WT or $T^{\Delta Gpx4/\Delta Gpx4}$ mice. Splenic cells were analyzed on 5 d after injection. Ns, not significant (Student's *t* test). Data are representative of four (A and B), three (E), and two (C, D, and F) independent experiments.

T cells die by ferroptosis in the absence of Gpx4

Earlier studies have suggested that Gpx4 inactivation in murine fibroblasts result in apoptosis-inducing factor (AIF)-mediated cell death as a consequence of lipid peroxide accumulation catalyzed specifically by 12/15-lipoxygenase in vitro (Seiler et al., 2008; Schneider et al., 2010). To investigate the survival of $T^{\Delta Gpx4/\Delta Gpx4}$ cells, we cultured peripheral T cells in vitro and monitored their viability. Both stimulated CD4+ and CD8+ splenocytes endured massive cell death at 37°C, which occurred as quickly as 2–3 h after incubation (Fig. 4 A). Notably, the exacerbated cell death was independent of TCR stimulation as similar results were obtained in unstimulated conditions and could not be further prevented by the addition of IL-2 (Fig. 4 B). We hypothesized that the reduction of T cells in the absence of Gpx4 was a result of the high oxygen levels in vitro (i.e., 21%), as compared with that of cells and tissues in vivo (i.e., 1–10%). To test this hypothesis, we cultured splenic T cells under hypoxic in vitro conditions (i.e., 1%).

Published March 30, 2015

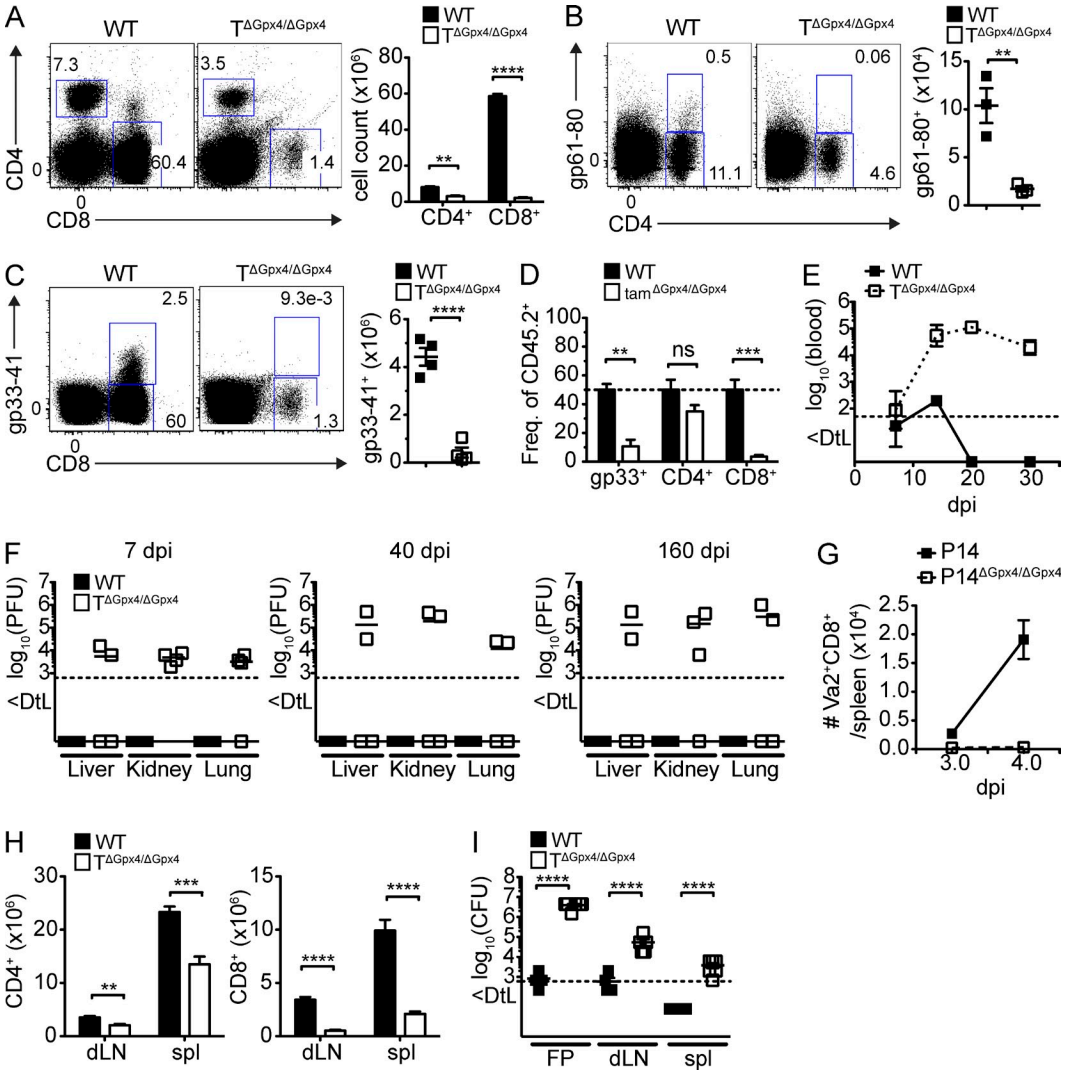

Figure 3. Gpx4-deficient T cells failed to expand following viral and parasite infection. WT and $T^{\Delta Gpx4/\Delta Gpx4}$ mice were infected with LCMV 200 plaque-forming units (pfu) WE i.v. and analyzed on 7 d after infection (dpi). (A) Flow cytometry of $CD4^+$ and $CD8^+$ T cells (left) and total numbers (right; $n = 4$ per group). (B and C) Flow cytometry (left) and absolute number (right) of gp61-80 tetramer positive $CD4^+$ (B) and gp33-41 tetramer positive $CD8^+$ (C) T cells ($n \geq 4$ per group). (D) Frequency of LCMV infected splenocytes from mixed BM chimeras generated by transfer of equal mixture (1:1) of BM stem cells from WT ($CD45.1^+$) and WT or $tam^{\Delta Gpx4/\Delta Gpx4}$ ($CD45.2^+$) mice into sublethally irradiated WT ($CD45.1^+$) mice. 8 wk after reconstitution, mice were treated with 2 mg of tamoxifen i.p. for 2 consecutive days, followed by infection with LCMV 200 pfu of WE strain, and analyzed at 10 dpi ($n = 3$ per group). (E) Viral titers in the blood of infected WT and $T^{\Delta Gpx4/\Delta Gpx4}$ mice over time. (F) Viral titers in the liver, lung, and kidney of infected WT and $T^{\Delta Gpx4/\Delta Gpx4}$ mice at 7 (left), 40 (middle), and 160 dpi (right; $n = 4$ per group). (G) Total number of $V\alpha2^+CD8^+$ T cells of WT ($CD45.1^+$) and $P14^{\Delta Gpx4/\Delta Gpx4}$ ($CD45.2^+$) mice that were adoptively transferred into WT ($CD45.1^+CD45.2^+$) mice and infected with LCMV-WE (1000 pfu) 2 h after transfer. Mice were analyzed at 3 and 4 dpi ($n = 5$ per group). (H and I) WT and $T^{\Delta Gpx4/\Delta Gpx4}$ mice were inoculated with 2×10^6 *L. major* stationary-phase promastigotes into the right hind footpad and analyzed at 10 wk after infection. Total number of $CD4^+$ (left) and $CD8^+$ (right) T cell in the draining LN (dLN), and spleen (spl; H). Parasite load in infected footpad (FP), dLN, and spleen were measured by limiting dilution analysis (I). Dotted line represents the limit of detection (DtL; $n = 6$ per group). Statistical significance is defined by Student's *t* test (**, $P \leq 0.01$; ***, $P \leq 0.001$; ****, $P \leq 0.0001$). Representative data are shown from four (A–C, E, and F), three (G), and two (D, H, and I) independent experiments.

The oxygen content delayed the cell death but was insufficient to prevent the death entirely (Fig. 4 C). The rapid death of Gpx4-deficient T cells was associated with a time-dependent increase in lipid peroxidation, as visualized using C11-$BODIPY^{581/591}$ dye that began at 2 h after incubation in $CD4^+$ T cells. Interestingly, lipid peroxidation was detected already after 0.5 h in $CD8^+$ T cells (Fig. 4 D), and correlated with the exacerbated cell death in $T^{\Delta Gpx4/\Delta Gpx4}$ cells. Addition of ebselen, an organo-selenic compound with a Gpx-like activity to scavenge lipid hydroperoxides, restored survival of $T^{\Delta Gpx4/\Delta Gpx4}$ cells dose dependently, confirming that the exacerbated death was due to uncontrolled lipid peroxidation occurring as a consequence of the lack of Gpx4 (Fig. 4 E).

Published March 30, 2015

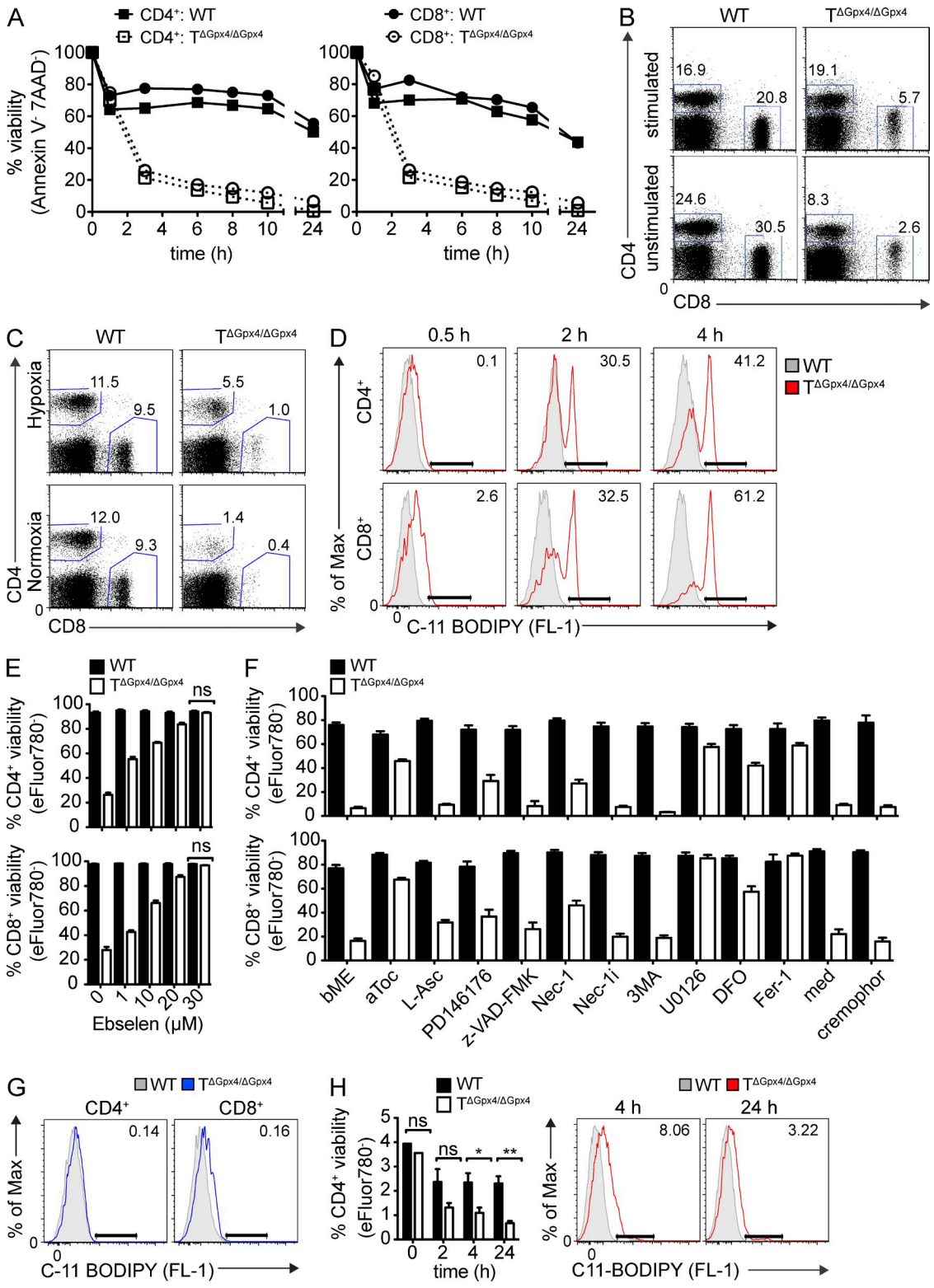

Figure 4. Gpx4-deficient T cells rapidly accumulate lipid peroxides and die by ferroptosis. (A) Frequencies of viability of CD4+ and CD8+ T cells from the LNs defined by Annexin V− and 7AAD− cells over time under stimulation with α-CD3 (5 µg/ml) and α-CD28 (2 µg/ml; left) or unstimulated (right) conditions (n = 3 per group). (B) Flow cytometry of viable CD4+ and CD8+ T cells LN cells distinguished by Annexin V−7AAD− (pregated) population after 4 h of culture at 37°C. Cells were stimulated with α-CD3 (5 µg/ml) and α-CD28 (2 µg/ml; top) or unstimulated (bottom) in the presence of IL-2 (20 ng/ml; n = 3 per group). (C) Flow cytometry of splenic CD4+ and CD8+ T cells cultured under normoxic (21% O_2) or hypoxic (1% O_2) conditions for 5 h at 37°C (n = 4 per group). (D) Accumulation of lipid peroxidation in CD4+ and CD8+ T cells determined by C11-BODIPY$^{581/591}$ (2 µM) at 0.5, 2, and 4 h after

Published March 30, 2015

We then attempted to rescue the T cell survival by testing a series of established inhibitors of classical cell death pathways and antioxidants, including inhibitors of a newly described iron-dependent cell death, ferroptosis (Dixon et al., 2012). The viability of Gpx4-deficient T cells was similar whether culturing whole splenocytes or MACS beads-sorted T cells (unpublished data). Cell death was not prevented by inhibitors of autophagy (3-methyladenine; 3MA), necroptosis (receptor-interacting protein 1 [RIP-1] inhibitor Necrostatin-1), or apoptosis (pan-caspase inhibitor z-VAD-fmk), which excluded major contributions of these pathways to the cell death induced by Gpx4 deficiency in vitro (Fig. 4 F). Consistent with the known function of Gpx4 in mitigating oxidative stress, the survival of both $CD4^+$ and $CD8^+$ T cells was prolonged by the addition of 12/15-lipoxygenase inhibitor PD146176 and α-tocopherol (aToc), the most abundant form of vitamin E known as a lipid-soluble antioxidant localized in the cell membrane, whereas the water-soluble antioxidant vitamin C did not have any effect (Fig. 4 F). Notably, addition of extracellular iron chelator deferoxamine (DFO), and ferroptosis inhibitor ferrostatin-1 (Fer-1) abolished the cell death in Gpx4-deficient T cells (Fig. 4 F) and prevented the up-regulation of C11-$BODIPY^{581/591}$ (Fig. 4 G), suggesting that the cell death involved ferroptosis. Indeed, RAS–RAF–MEK signaling has been shown to be required for erastin-induced ferroptosis of tumor cells (Yagoda et al., 2007). Consistent with this finding, we observed that the MEK inhibitor U0126 restored the survival of Gpx4-deficient T cells. Additionally, concurring with in vitro results, in vivo activation of T cells using α-CD3 resulted in increased lipid peroxidation and decreased T cell number in $T^{\Delta Gpx4/\Delta Gpx4}$ mice already after 4 h (Fig. 4 H), indicating rapid cell death after T cell activation. Similar results were obtained after injection of *Staphylococcus* enterotoxin B superantigen (not depicted). Collectively, these results suggest that T cells lacking Gpx4 die by ferroptosis rapidly after T cell activation.

Given previous in vitro results using a chemical inhibitor of 12/15-lipoxygenase (Fig. 4 F) and the aforementioned results suggesting that lipid peroxidation is responsible for the death of T cells lacking Gpx4, we crossed 12/15-lipoxygenase–deficient ($Alox15^{-/-}$) and $T^{\Delta Gpx4/\Delta Gpx4}$ mice to investigate peripheral T cell homeostasis in the absence of both *Alox15* and *Gpx4* genes in vivo (Seiler et al., 2008; Schneider et al., 2010). T cell numbers were comparable in single and double knockout mice demonstrating that *Alox15* is not responsible for the disappearance of $CD8^+$ T cells in Gpx4-deficient mice (Fig. 5 A). Absence of *Alox15* only slightly increased virus-driven expansion of $CD8^+$ T cells in $T^{\Delta Gpx4/\Delta Gpx4}$ but failed to reconstitute to WT levels (Fig. 5 B). Moreover, we found that the absence of RIP3 did not rescue T cell expansion in LCMV-infected $T^{\Delta Gpx4/\Delta Gpx4/}Ripk3^{-/-}$ mice (Fig. 5 C). The lack of necroptotic pathway was further confirmed by the results obtained by inhibition of RIP1 (Fig. 5, D and E). These findings together suggested that Gpx4 deletion-induced T cell death is not caused by classical cell death pathways but by lipoperoxide-mediated pathways involving ferroptosis. Furthermore, *Alox15* is not the main enzyme involved in the accumulation of toxic lipid peroxides but rather other nonenzymatic oxidation or cellular ROS mechanisms are involved in this process, with no involvement of necroptotic cell death during viral infection in vivo.

Dietary vitamin E can restore viability, antiviral T cell expansion, and clearance of LCMV in susceptible $T^{\Delta Gpx4/\Delta Gpx4}$ mice

Based on the observation that the presence of aToc rescued the survival of Gpx4-deficient T cells (Fig. 4 F), we investigated the effects of vitamin E in vivo. We fed WT and $T^{\Delta Gpx4/\Delta Gpx4}$ mice with low vitamin E ($VitE^{lo}$; <10 mg/kg), chow (50 mg/kg) or excess vitamin E ($VitE^{hi}$; 500 mg/kg) for 3 wk and analyzed the mice at 6 wk of age. In agreement with aToc-mediated protection from death in vitro, dietary supplementation restored peripheral $CD8^+$ T cell survival in $T^{\Delta Gpx4/\Delta Gpx4}$ mice (Fig. 6 A). We next infected mice with LCMV-WE and monitored T cell expansion and viral clearance. Groups of WT and $T^{\Delta Gpx4/\Delta Gpx4}$ mice were fed chow or high vitamin E for 3 wk before infection, and analyzed at 7 d after infection (dpi). $T^{\Delta Gpx4/\Delta Gpx4}$ mice fed with high vitamin E showed a partial recovery of virus-specific $CD8^+$ T cells (Fig. 6 B) with a normal distribution of $CD127^-KLRG\text{-}1^+$ short-lived effector cells (SLECs) and $CD127^+KLRG\text{-}1^-$ memory precursor effector cells (MPECs) cells (not depicted), and strikingly increased the capability of viral clearance (Fig. 6 C). These data show that vitamin E is a potent lipid antioxidant that can potentially compensate for the lack of Gpx4.

Next, we investigated whether Gpx4 was required for a secondary T cell response. WT and $tam^{\Delta Gpx4/\Delta Gpx4}$ mice were infected with LCMV-WE, and Gpx4 was deleted 10 wk later by tamoxifen administration followed by infection with *L. monocytogenes* expressing the LCMV gp33 epitope (Lm-gp33; 5×10^4 cfu). Gpx4 deletion was confirmed in the mRNA (Fig. 6 D) and in lysates of $CD8^+$ T cells by Western blot (Fig. 6 E). On day 4 after rechallenge, both $tam^{\Delta Gpx4/\Delta Gpx4}$ and WT mice mounted a potent and comparable gp33-specific $CD8^+$ T cell response (Fig. 6 F) that resulted in sterile clearance

incubation at 37°C ($n = 3$ per group). (E) Percent viability of stimulated $CD4^+$ (left) and $CD8^+$ (right) splenic T cells after 4 h at 37°C with various concentrations of ebselen ($n = 3$ per group). (F) Frequencies of viable ($eFluor780^-$) splenic $CD4^+$- (left) and $CD8^+$-stimulated (right) T cells treated with antioxidants or cell death pathway inhibitors for 24 h at 37°C ($n = 4$ per group). (G) C11-$BODIPY^{581/591}$ (FL-1) accumulation in stimulated $CD4^+$ and $CD8^+$ T cells, treated with ferrostatin-1 (Fer-1; 10 µM) for 4 h ($n = 3$ per group). (H) Total number of splenic $CD4^+$ T cells at 0, 2, 4, and 24 h after intravenous injection of α-CD3 antibody (1 µg; left) and lipid peroxidation assessed by C11-$BODIPY^{581/591}$ at 4 and 24 h after injection (right; $n = 3$ per group). The data are representative of at least five (A, B, and F), three (D, E, and G), and two (H) independent experiments. Statistical significance is defined by Student's *t* test (*, $P \le 0.1$; **, $P \le 0.01$).

Published March 30, 2015

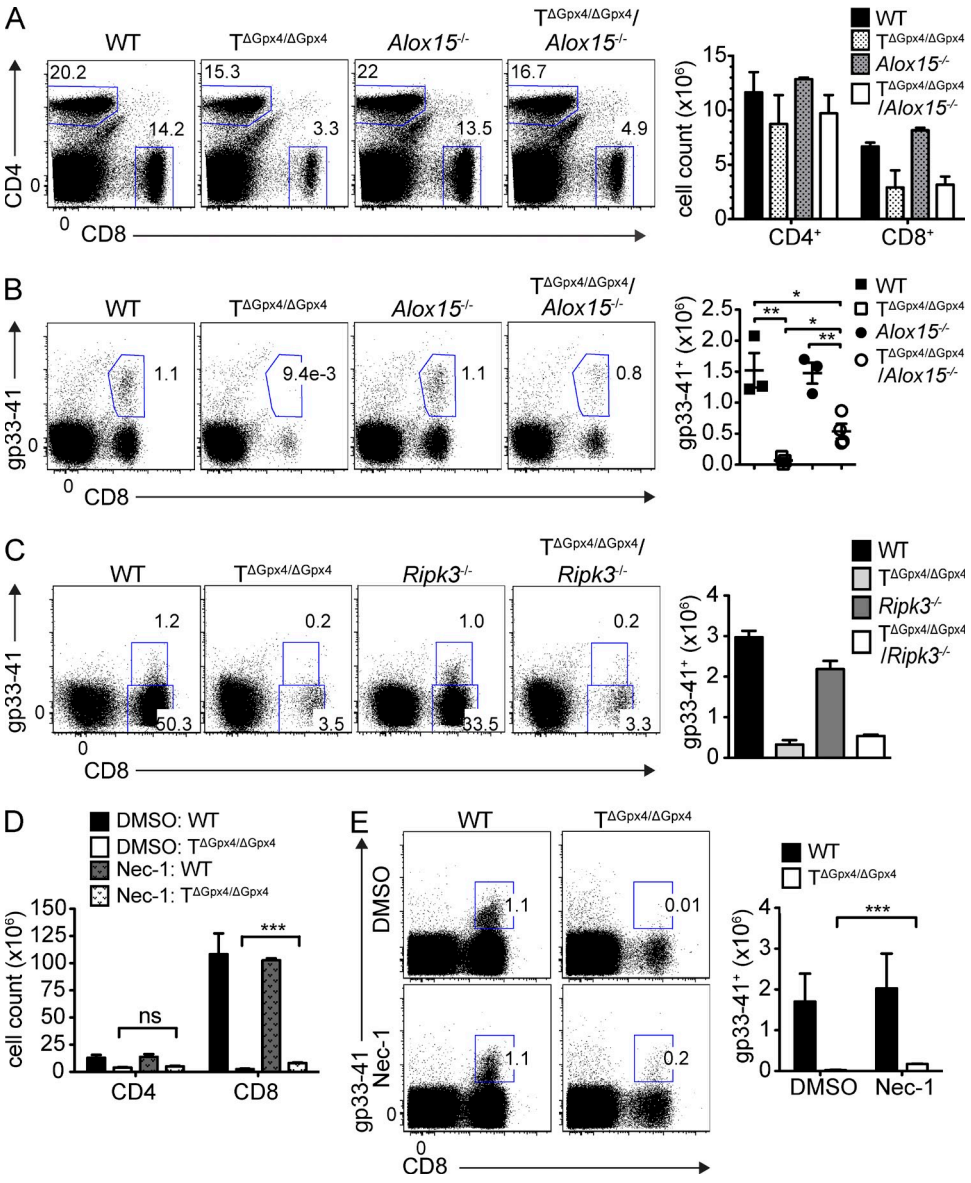

Figure 5. 12/15-lipoxygenase does not restore viability of Gpx4 deficient T cells. (A) Splenic CD4+ and CD8+ T cell population (left) and numbers (right) of WT, $T^{\Delta Gpx4/\Delta Gpx4}$, 12/15-lipoxygenase (*Alox15*$^{-/-}$), and $T^{\Delta Gpx4/\Delta Gpx4}$ crossed with 12/15-lipoxygenase ($T^{\Delta Gpx4/\Delta Gpx4}$/*Alox15*$^{-/-}$; $n = 3$ per group of 6 wk old mice). Flow cytometry (left) and total number (right) of gp_{33-41} tetramer specific CD8+ cells from LCMV-infected spleens of WT, $T^{\Delta Gpx4/\Delta Gpx4}$, *Alox15*$^{-/-}$, and $T^{\Delta Gpx4/\Delta Gpx4}$/*Alox15*$^{-/-}$ (B; $n \geq 4$ per group). WT, $T^{\Delta Gpx4/\Delta Gpx4}$, *Ripk3*$^{-/-}$, and $T^{\Delta Gpx4/\Delta Gpx4}$/*Ripk3*$^{-/-}$ (C; $n = 3$ per group) at 7 dpi. (D and E) Necrostatin-1 (Nec-1; 1.65 mg/kg) was injected daily beginning from 2 d before infection with LCMV 200 pfu WE strain. Total number of splenic CD4+ and CD8+ T cells (D) and gp33-41 tetramer specific CD8+ T cells (E) at 7 dpi ($n = 3$ per group). Representative data are shown from two independent experiments. *, $P \leq 0.05$; **, $P \leq 0.01$; ***, $P \leq 0.001$ (two-tailed Student's *t* test).

of bacteria, whereas groups of mice undergoing primary infection were all moribund and had to be euthanized (not depicted). Excess dietary vitamin E supplementation did not affect the rapid CD8+ T cell expansion to secondary infection quantitatively but qualitatively by increasing the frequency of central memory cells ($CD62L^+CD127^+$) in WT mice and both effector memory ($CD62L^-CD127^+$) and central memory cells in $tam^{\Delta Gpx4/\Delta Gpx4}$ mice (Fig. 6 G). Collectively, these results suggest that Gpx4 is essential for the primary but not a secondary T cell response.

DISCUSSION

It has become increasingly evident that naive, activated, and memory T cells are regulated by different metabolic signals including nutrient availability, intracellular metabolites, and metabolic products such as NADPH and ROS (Wang and Green, 2012; MacIver et al., 2013; Pearce and Pearce, 2013). TCR stimulation has been shown to induce production of discrete species of ROS (i.e., hydrogen peroxide and superoxide anion), involving a phagocyte type NADPH oxidase expressed by T cells and the FAS pathway (Devadas et al.,

Published March 30, 2015

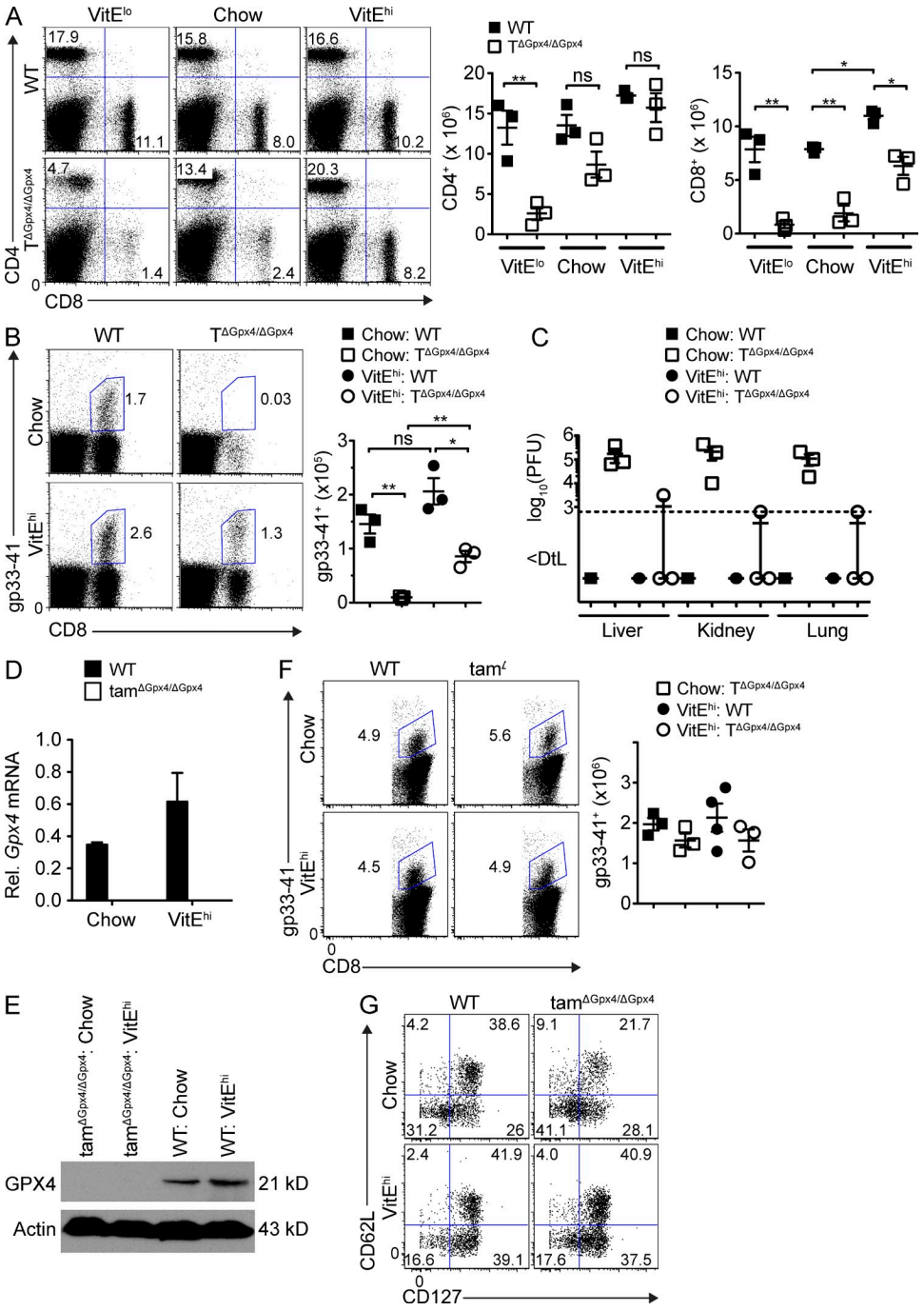

Figure 6. Vitamin E rescues CD8⁺ T cell defect and restores viral clearance. Mice fed with vitamin E low (VitE^{low}; <10 mg/kg), chow (50 mg/kg), or vitamin E high (VitE^{hi}; 500 mg/kg) for 3 wk. (A) Flow cytometry (left) and absolute number of splenic CD4⁺ (middle) or CD8⁺ T cells (right) in WT and T$^{\Delta Gpx4/\Delta Gpx4}$ mice after 3 wk of diet supplementation (n = 3 per group of 6-wk-old mice). (B) Flow cytometry (left) and total number (right) of gp33-41 tetramer specific CD8⁺ T cells in the spleen (n = 3 per group) at 7 dpi with LCMV WE 200 pfu. (C) Viral titers of LCMV (WE 200 pfu) infected mice in the liver, lung, and kidney (n = 3 per group) at 7 dpi. (D and E) Quantification of *Gpx4* mRNA levels in splenic MACS sorted CD8⁺ T cells. Expression was normalized to *G6pdx* mRNA levels. (E) Western blot of GPX4 expression withactin as loading control in splenic MACS sorted CD8⁺ T cells. (F) Flow cytometry of splenocytes infected with LCMV WE (200 pfu), followed by Gpx4 deletion with tamoxifen (2 mg for 2 d) and infection with *L. monocytogenes* expressing the LCMV gp33 epitope (LM-gp33; 5 × 10^4 cfu) at 69 dpi. Mice were given vitamin E diet 1 wk before LM-gp33 infection. Analysis at 4 dpi with LM-gp33 ($n \geq 5$ per group). (G) Expression of CD62L and CD127 from splenocytes as in (F). Representative data are shown from three (A–C) and two (D–G) independent experiments. *, $P \leq 0.05$; **, $P \leq 0.01$ (Student's t test).

Published March 30, 2015

2002; Jackson et al., 2004). Moreover, mitochondria are a major source of ROS and mitochondrial ROS is essential for T cell activation, expansion and effector function (Sena et al., 2013; Yi et al., 2006).

Although Gpx4 is known for its role as an important phospholipid hydroperoxide scavenger (Thomas et al., 1990), we have shown that Gpx4 is essential for the cell-intrinsic mechanism to prevent ROS-mediated membrane phospholipid peroxidation and death after T cell activation. T cell expansion and generation of effectors after viral infection was completely abrogated in the absence of Gpx4. Gpx4-deficient T cells died within a few hours before cell division after activation by *Staphylococcus* superantigen or α-CD3 in vivo (Fig. 4 H). The failure to undergo homeostatic expansion and loss of Gpx4-deficient T cells after transfer into lymphopenic mice or in mixed BM chimeras implies that Gpx4 is also required for survival of dividing T cells under noninflammatory conditions. TCR interactions with self-ligands presented by MHC class I and II are known to be required for peripheral survival of $CD8^+$ and $CD4^+$ T cells, respectively. Absence of such interactions results in death of $CD8^+$ T cells within a few days, whereas $CD4^+$ T cells survive with a half-life of months (Rooke et al., 1997; Tanchot et al., 1997; Selin et al., 1999), which may explain why Gpx4 is predominantly required for survival of peripheral $CD8^+$ T cell in homeostasis. The remaining $CD8^+$ T cells of $T^{\Delta Gpx4/\Delta Gpx4}$ mice showed no changes in expression of activation markers (Fig. 1 H), indicating that the loss of T cells was not a result of hyperactivation or hyperproliferation, as for instance observed in mice with a defect in regulatory T cells.

In contrast to conventional T cells, absence of Gpx4 did not affect expansion of regulatory T cells. T reg cells are known to secrete more thioredoxin-1, an antioxidant, than effector T cells, and therefore may be more resistant to ROS-induced damage (Mougiakakos et al., 2011). Absence of Gpx4 in hematopoietic precursors also did not interfere with normal thymic T cell development, including massive T cell proliferation at the DN3/DN4 stage and selection at DP stage (Fig. 2, A and C), despite high expression of Gpx4 in thymocytes.

The abrogated primary response and chronic LCMV infection in $T^{\Delta Gpx4/\Delta Gpx4}$ did not allow us to study the requirement of Gpx4 for a bonafide memory/recall response. To circumvent this problem, we capitalized on generation of tamoxifen-inducible knockouts ($tam^{\Delta Gpx4/\Delta Gpx4}$) and depletion of Gpx4 in mice with intact memory to LCMV directly before secondary infection with recombinant *Listeria* encoding the LCMV-gp33. Similar to thymocyte development, Gpx4 was dispensable for an efficient and protective recall response. Emerging studies highlight that distinct metabolic pathways contribute to the fate decisions of effector and memory T cells (Wang and Green, 2012; MacIver et al., 2013; Pearce and Pearce, 2013). To generate energy, effector cells use aerobic glycolysis, whereas memory cells rely on oxidative phosphorylation. When compared with effector cells, memory cells have a greater capacity for extramitochondrial energy generation and produce less superoxide (van der Windt et al., 2012), which may explain why they can survive without Gpx4.

After immune responses to infections, T cell populations are controlled and maintained by programmed cell death, one of which is initiated by the death receptor ligation, involving Fas-associated death domain protein (FADD) and caspase 8 (Ashkenazi and Dixit, 1998). Although apoptosis has long been considered the primary form of programmed cell death, recent studies have identified that necroptosis can also occur by inactivation of caspase 8 and complex formation of RIP kinase 1 and 3 (Cho et al., 2009; Declercq et al., 2009). T cells lacking caspase 8 or its adaptor protein FADD exhibit defective T cell homeostasis, clonal expansion, contraction, and antiviral responses (Walsh et al., 1998; Ch'en et al., 2011). Similar to the T cell phenotype in $T^{\Delta Gpx4/\Delta Gpx4}$ mice, mice that undergo necroptotic cell death also display a decrease in primarily $CD8^+$ T cell populations (Ch'en et al., 2011). However, we found that the absence of *RIPk3* did not rescue T cell expansion in LCMV-infected $T^{\Delta Gpx4/\Delta Gpx4/}$ $Ripk3^{-/-}$ mice, which demonstrated that necroptosis is not involved in the death of activated *Gpx4*-deficient T cells. Concomitant to these findings, Gpx4-deficient T cell cultured with pharmacological inhibitors of autophagy, apoptosis, and necroptosis, such as 3-methyladenine, z-VAD-FMK, a pan-caspase inhibitor, and necrostatin-1, which binds to RIPk1 and blocks DR-induced necroptosis (Degterev et al., 2005), failed to prevent the cell death. We therefore conclude that the toxic lipid peroxidation in T cells does not involve conventional cells death pathways. In line with the in vitro results, an unexpected finding was that the Gpx4-deficient T cell death was triggered in vitro irrespective of TCR stimulation. As it has been reported that normoxia increases oxygen radicals and promotes hydrogen peroxides generation (Fan et al., 2008), the effect in vitro suggests that the Gpx4-deficient T cells acquire damage already ex vivo as a consequence of high oxygen levels in normoxic conditions, which provoked the exacerbated cell death in vitro as compared with in vivo homeostasis.

Vitamin E is known to function as a lipid-soluble antioxidant that eliminates peroxyl radicals and prevents the propagation of lipid peroxidation (Tappel, 1972). In contrast, vitamin C is a water-soluble antioxidant that cannot directly function on the lipid bilayer (Niki et al., 1985). From our results, we observed that addition of vitamin E to Gpx4-deficient T cells enhanced the survival of splenic T cells in vitro, and further restored peripheral $CD8^+$ T cell homeostasis and antiviral T cell expansion in vivo; however, the addition of vitamin C did not rescue the survival of Gpx4-deficient T cells. This ability of vitamin E to promote the survival of $T^{\Delta Gpx4/\Delta Gpx4}$ cells indicates the involvement of oxidized lipids in death of activated T cells lacking Gpx4, an idea further supported by the presence of accumulated lipid peroxidation in activated $T^{\Delta Gpx4/\Delta Gpx4}$ cells. Previously, 12/15-lipoxygenase has been implicated in the death of *Gpx4*-deficient fibroblasts in vitro (Seiler et al., 2008). In agreement with these findings, pharmacological inhibition of 12/15-lipoxygenase partially protected

Published March 30, 2015

them from cell death. However, our findings in vivo led us to conclude that solely knocking out 12/15-lipoxygenase is insufficient to prevent lipid peroxidation, as $T^{\Delta Gpx4/\Delta Gpx4}$/*Alox15*$^{-/-}$ mice failed to rescue peripheral T cell viability or restore antiviral T cells upon LCMV infection. Instead, we speculate that 5-lipoxygenase may be responsible for toxic lipid peroxidation in T cells lacking *Gpx4* in the presence or absence of 12/15-lipoxygenase (Los et al., 1995; Cook-Moreau et al., 2007).

Erastin-induced ferroptotic death of RAS mutant tumor cells has been reported to prevent glutamate-induced neurotoxicity (Dixon et al., 2012), regulated by Gpx4 (Yang et al., 2014). Our results show that Fer-1 prevented lipid peroxidation and sustained survival of Gpx4-deficient T cells. Moreover, inhibition of iron availability by the iron-chelating agent, DFO, prevented T cell death. No differences were found in expression of the transferrin receptor (CD71) and ferroportin, the major pathways for iron import and export, respectively, on $CD8^+$ T cells from naive and LCMV-infected mice, indicating that iron transport is not affected in the absence of Gpx4. Possibly the intracellular iron oxidation status (Fe^{2+}/Fe^{3+}) availability in vivo plays an important role in the maintenance of cell survival, especially in Gpx4-deficient conditions. $T^{\Delta Gpx4/\Delta Gpx4}$ cells cultured in Iscove's Modified Dulbecco Media that lacks iron consistently underwent cell death.

Although the precise mechanism by which Gpx4 deficiency dampens the cell survival is largely uncertain, the involvement of RAS–RAF–MEK signaling pathway has been implicated in ferroptotic cell death (Yagoda et al., 2007). Indeed, activation of the MAP kinase ERK pathway by TCR stimulation plays a key role in T cell fate decision and responses (Smith-Garvin et al., 2009). ERK1/2 phosphorylation upon TCR triggering depends on the generation of hydrogen peroxide and stimulates glutamine uptake (Devadas et al., 2002; Carr et al., 2010). Interestingly, our results indicated that inhibition of ERK1/2 activation by blockade of MEK1/2 also prevented Gpx4-deficient T cell death in culture, implicating deregulated ERK activation caused by lipid peroxidation and further strengthening the idea that Gpx4-deficient T cells undergo ferroptosis, Erastin has been reported to inhibit the x_c^- cystine/glutamate transporter and thereby to inhibit cystine uptake and cause ferroptotic cell death (Dixon et al., 2012). Cystine in the extracellular space is transported exclusively by the x_c^- and converted to cysteine, which facilitates the synthesis of intracellular glutathione (GSH), a major cellular antioxidant (Fahey and Sundquist, 1991). Because naive T cells do not express x_c^-, they are metabolically dependent on APCs to maintain homeostatic balance and undergo T cell activation and proliferation (Angelini et al., 2002). Although it has become widely understood that T cells can in fact up-regulate x_c^- upon activation, T cells in the early stages of activation still require cysteine from other sources (Levring et al., 2012). As we report that the $T^{\Delta Gpx4/\Delta Gpx4}$ T cells undergo ferroptotic cell death in the absence of x_c^-, we speculate that ferroptosis is not exclusively triggered by blocking x_c^-. The mechanism by which ferroptosis occurs in T cells remain uncertain.

Collectively, our results establish a pivotal role of Gpx4 for the survival and expansion of recently activated T cells by prevention of lipid peroxidation and ferroptotic cell death, a metabolic pathway also used by tumor cells for survival (Yang et al., 2014). Our data also demonstrate a beneficial role of dietary supplementation of high-dose vitamin E for treatment of genetic disorders or environmental cues driving lipid peroxidation and related pathologies.

MATERIALS AND METHODS

Mice. $T^{\Delta Gpx4/\Delta Gpx4}$ and $tam^{\Delta Gpx4/\Delta Gpx4}$ mice were generated by crossing *Gpx4*$^{fl/fl}$ mice (C57BL/6; $n > 8$; Seiler et al., 2008) to *Cd4*-cre (JAX; Lee et al., 2001) and *Ert2*-Cre (Hameyer et al., 2007), respectively. Strains of *Alox15*$^{-/-}$ (JAX; Sun and Funk, 1996), *Ripk3*$^{-/-}$ mice (obtained originally from the late J. Tschopp with kind permission of Vishva M. Dixit, Genentech, South San Francisco, CA; Newton et al., 2004), and P14 (JAX; Pircher et al., 1989) were crossed to $T^{\Delta Gpx4/\Delta Gpx4}$ to generate $T^{\Delta Gpx4/\Delta Gpx4}$/*Alox15*$^{-/-}$, $T^{\Delta Gpx4/\Delta Gpx4}$/*Ripk3*$^{-/-}$, and $P14^{\Delta Gpx4/\Delta Gpx4}$, respectively. All mice were crossed for more than eight generations to C57BL/6. For in vivo vitamin E supplementation, age- and sex-matched littermates were fed with vitamin E high (500 mg/kg), chow (50 mg/kg), or deficient (<10 mg/kg) food for 3 consecutive weeks in $T^{\Delta Gpx4/\Delta Gpx4}$ mice at 3 wk of age and for 1 wk in $tam^{\Delta Gpx4/\Delta Gpx4}$ mice at 6 wk of age (ssniff Spezialdiäten GmbH). Gpx4 was deleted by 2 mg tamoxifen i.p. administration for 2 d. Animals were housed and maintained in specific pathogen–free conditions at BioSupport. All recipient mice were age- and sex-matched from the ages 4–20 wk. All animal experiments were performed according to the institutional guidelines and Swiss federal regulations, and were approved by the local ethics committee of Kantonales Veterinaramt in Zurich, Switzerland (permission no. 148/2008).

RNA, DNA, and protein analysis. Thymic DP, CD4 SP, and CD8 SP were sorted with FACSAria IIIu (BD). Splenic $CD4^+$, $CD8^+$, and $CD90^+$ T cells were isolated using CD4 (L3T4), CD8a (Ly-2), and CD90.2 (Thy1.2) microbeads, respectively, from MACS (Miltenyi Biotec). Total RNA was extracted using TRI Reagent (Invitrogen), followed by reverse transcription using GoScript RT (Promega). Total genomic DNA was precipitated by isopropanol at 56°C for 1 h. Quantitative real-time RT-PCR was performed using Brilliant SYBR Green (Stratagene) on an i-Cycler (Bio-Rad Laboratories) according to manufacturer's protocol. Relative *Gpx4* expression was normalized to housekeeping genes *G6pdx*-F (5′-CTACAGGTTCAGATGATGTC-3′) and *G6pdx*-R (5′-CAGCTTCTCCTTCTCCATTG-3′) or *Gapdh*-F (5′-GGGTGTGAACCACGAGAAAT-3′) and *Gapdh*-R (5′-CCTTCCACAATGCCAAAGTT-3′). Primer sequences are as follows: *Gpx4*-F (5′-GCAACCAGTTTGGGAGGCAGGAG-3′), *Gpx4*-R (5′-CCTCCATGGGACCATAGCGCTTC-3′), *Gpx4*$^{fl/fl}$-F (5′-CTCTTTAAGGACAGCCAGTG-3′), and *Gpx4*$^{fl/fl}$-R (5′-GCCCATAGTCCTAAGATCAC-3′).

Purified splenic T cells were lysed on ice with RIPA buffer (20 mM Tris-HCl, pH 7.5, 150 mM NaCl, 5 mM EDTA, 1 mM Na_3VO_4, 1% Triton X-100, supplemented with protease inhibitor [Sigma-Aldrich] and phosphatase inhibitor [Sigma-Aldrich]), and spun for 10 min at 4°C. Protein concentrations were determined using a protein assay (Bio-Rad Laboratories). Antibodies for GPX4 (R&D Systems) and Actin (C-11; Santa Cruz Biotechnology, Inc.) were used.

Flow cytometry. For analysis of cell surface markers, cells were stained in PBS containing 2% heat-inactivated FBS with 2 mM EDTA supplementation, unless noted otherwise. Antibodies used were as follows: CD4-PerCP/Cy5.5, CD8α-APC, and CD127-APC (BioLegend); CD4-PE and CD44-PE (BD); CD62L-FITC, CD25-PE, CD45.2-FITC, and CD45.1-PE (eBioscience). Foxp3-APC and eFluor780 (eBioscience), Annexin V-FITC, and 7-AAD (BD) were stained according to the manufacturer's instructions. Cells were analyzed with FACSCalibur or FACSCanto II flow cytometry (BD) using FlowJo software (Tree Star).

Published March 30, 2015

Generation of mixed BM chimera. Donor BM cells were isolated aseptically from the femurs and tibias of 8-wk-old WT (CD45.2$^+$), T$^{\Delta Gpx4/\Delta Gpx4}$ (CD45.2$^+$), and C57BL/6 (CD45.1$^+$) mice. C57BL/6 WT (CD45.1$^+$CD45.2$^+$) male mice (8 wk old) received a lethal dose of whole body irradiation and were transfused by intravenous injection of equal numbers of CD45.1 and CD45.2 donor BM cells. For the generation of tamoxifen-inducible chimeras, WT (CD45.2$^+$), and tam$^{\Delta Gpx4/\Delta Gpx4}$ (CD45.2$^+$) mice were pretreated twice with 2 mg tamoxifen (Sigma-Aldrich) i.p. At day 5 after induction, BM cells were isolated and reconstituted with equal ratios of CD45.1 and CD45.2 into lethally irradiated C57BL/6 WT (CD45.1$^+$) female mice (6 wk old). Recipient mice received normal chow and water containing antibiotics for 6 wk after transplantation. Mice were analyzed 7 wk after reconstitution.

Homeostatic T cell expansion in *Rag*1-deficient mice. Congenically marked thymocytes from T$^{\Delta Gpx4/\Delta Gpx4}$ (CD45.2$^+$) and C57BL/6 (CD45.1$^+$) were mixed at equal ratio, and 5×10^6 cells were injected i.v. into *Rag*1-deficient mice. Mice were bled at 1, 5, and 7 d after transfer and analyzed by flow cytometry.

Expansion of regulatory T cells by IL-2 immune complex injection. Recombinant mouse IL-2 (eBioscience) was mixed with anti–IL-2 (clone JES6-1A12) and incubated at 37°C for 20 min. Mice were injected on day 0, 1, and 2, and analyzed on day 5.

LCMV, *Listeria monocytogenes*, and *Leishmania major* infection. The LCMV glycoprotein peptides gp_{33-41} (GP33 peptide, KAVYNFATM) and gp_{61-80} (GP61, GLNGPDIYKGVYQFKSVEFD) were kindly provided by the National Institutes of Health (Bethesda, MD). Mice were infected with LCMV-WE (200 pfu) i.v. LCMV-infected mice were bled and the blood was diluted 1/5 with MEM supplemented with 2% FBS and heparin. Nonlymphoid organs were harvested in 1 ml of MEM 2% FBS and lysed using a tissue lyser (Retsch GmbH) for viral load determination. Blood and organs were stored at −80°C until analysis. Plaque assays were performed as described previously on MC57 cells (Planz et al., 1997). For the secondary rechallenge experiments, WT and tam$^{\Delta Gpx4/\Delta Gpx4}$ mice were injected i.v. with 200 pfu of LCMV WE. After 69 dpi, mice were given high vitamin E or chow diet until the end of the experiments. Gpx4 was deleted with intraperitoneal injection of tamoxifen. Frozen stocks of *L. monocytogenes* that express gp_{33-41} epitope of LCMV (Lm-gp33) were grown in brain–heart infusion broth. Bacterial cultures were grown to mid-log phase and measured the optical density at 600 nm. Mice were rechallenged with 5×10^4 cfu i.v. Injected bacterial numbers were determined by overnight culture of bacterial sample on brain–heart infusion agar plates at 37°C. Mice were analyzed 4 d later. Bacterial titers were quantified by plating serial dilutions on brain–heart infusion agar plates.

L. major parasite (MHOM/IL/81/FEBNI) were grown in Schneider's *Drosophila* Medium (Invitrogen) with 20% FBS and 100 U/ml penicillin 6-potassium and 100 µg/ml streptomycin sulfate. Mice were injected with 2×10^6 metacyclic promastigote parasites into the right hind footpad, and were analyzed 10-wk after infection. To quantify parasite load in lesions, single-cell suspensions were plated on 96-well plates in triplicates of threefold serial dilutions and were cultured at 27°C for 7 d.

Expansion of LCMV specific P14$^{\Delta Gpx4/\Delta Gpx4}$ T cells. CD8$^+$ T cells were isolated from the spleen of P14 (CD45.1$^+$) and P14$^{\Delta Gpx4/\Delta Gpx4}$ (CD45.2$^+$) by CD8 negative selection (Miltenyi Biotec). Cells mixed at equal ratio (1:1 ratio; 10^6 cells) were transferred into naive recipient mice (CD45.1$^+$CD45.2$^+$). The recipient mice were infected with LCMV-WE (1,000 pfu) 2 h after transfer, and splenocytes were analyzed at day 3 and 4 after transfer. P14 cells were distinguished by Vα2$^+$CD8$^+$ cells.

Viability assays. T cells were cultured with plate bound α-CD3 (5 µg/ml) and soluble α-CD28 (2 µg/ml) with IL-2 (20 ng/ml) at 37°C in IMDM (Invitrogen) media supplemented with 10% FCS (Invitrogen) unless stated otherwise. All reagents were purchased from Sigma-Aldrich except otherwise stated. The following small molecule inhibitors were tested in threefold dilution series: β-mercaptoethanol (b-ME, 50 µM; Invitrogen), α-tocopherol (aToc, 100 µM), ascorbic acid (L-Asc, 10 µM), PD146176 (1 µM), z-VAD-FMK (100 µM; R&D Systems), Necrostatin-1 (Nec-1, 100 µM; Merck), Necrostatin-1 inactive control (Nec-1i, 100 µM; Merck), 3-methyladenine (3MA, 10 µM), U0126 (100 µM), deferoxamine (DFO, 400 µM), and Ferrostatin-1 (Fer-1, 10 µM; ChemBridge). Ebselen was purchased from Sigma-Aldrich. Cremophor EL (Sigma-Aldrich) was used to solubilize α-tocopherol in aqueous solution according to the manufacturer's protocol. Whole splenocytes and peripheral LNs were isolated and treated in vitro with plate-bound α-CD3 (5 µg/ml; homemade), soluble α-CD28 (2 µg/ml; BioLegend), and IL-2 (20 ng/ml; homemade) at 37°C with 5% CO_2.

For T cell viability analysis in vivo, mice were injected with α-CD3 (1 µg; eBioscience) i.v., and splenocytes were isolated for analysis.

Visualization of lipid peroxidation. Splenocytes (10^6 cells/well) were seeded on plate-bound α-CD3 (5 µg/ml; homemade) and were loaded with 2 µM C11-BODIPY$^{581/591}$ (Invitrogen) for 0.5, 2, and 4 h. BODIPY emission was recorded on FL-1. Data were collected from a minimum of 10,000 cells.

Hypoxic cell culture. Splenocytes were incubated in a hypoxia chamber gassed with 1% O_2 and 5% CO_2. Tissue culture incubator with ambient 21% O_2 and 5% CO_2 was used for normoxic controls. Cells were isolated and incubated with plate-bound α-CD3 (5 µg/ml; homemade) and soluble α-CD28 (2 µg/ml; BioLegend) at 37°C. FACS analysis was performed 5 h and 24 h after incubation. Cell viability was determined using Annexin V and 7AAD.

Statistical analysis. Two-tailed paired and unpaired Student's *t* tests were performed using Prism 5.0 (GraphPad software). *, $P < 0.05$; **, $P < 0.01$; ***, $P < 0.001$; ****, $P < 0.0001$.

We thank Jan Kisielow for helpful discussions, Iwana Schmitz and Luigi Tortola for technical advice, the ETH Flow Cytometry Core Facility for cell sorting, the National Institutes of Health Tetramer Facility for the providing GP33 tetramers and the BioSupport technicians for animal care.

This work was supported by SNF 310030B_141175/1 and ETH 0-2611-09.

The authors have no conflicting financial interests.

Submitted: 5 May 2014
Accepted: 10 March 2015

REFERENCES

Angelini, G., S. Gardella, M. Ardy, M.R. Ciriolo, G. Filomeni, G. Di Trapani, F. Clarke, R. Sitia, and A. Rubartelli. 2002. Antigen-presenting dendritic cells provide the reducing extracellular microenvironment required for T lymphocyte activation. *Proc. Natl. Acad. Sci. USA*. 99:1491–1496. http://dx.doi.org/10.1073/pnas.022630299

Ashkenazi, A., and V.M. Dixit. 1998. Death receptors: signaling and modulation. *Science*. 281:1305–1308. http://dx.doi.org/10.1126/science.281.5381.1305

Beck, M.A., D. Williams-Toone, and O.A. Levander. 2003. Coxsackievirus B3-resistant mice become susceptible in Se/vitamin E deficiency. *Free Radic. Biol. Med*. 34:1263–1270. http://dx.doi.org/10.1016/S0891-5849(03)00101-1

Brownlee, M. 2001. Biochemistry and molecular cell biology of diabetic complications. *Nature*. 414:813–820. http://dx.doi.org/10.1038/414813a

Carr, E.L., A. Kelman, G.S. Wu, R. Gopaul, E. Senkevitch, A. Aghvanyan, A.M. Turay, and K.A. Frauwirth. 2010. Glutamine uptake and metabolism are coordinately regulated by ERK/MAPK during T lymphocyte activation. *J. Immunol*. 185:1037–1044. http://dx.doi.org/10.4049/jimmunol.0903586

Ch'en, I.L., J.S. Tsau, J.D. Molkentin, M. Komatsu, and S.M. Hedrick. 2011. Mechanisms of necroptosis in T cells. *J. Exp. Med*. 208:633–641. http://dx.doi.org/10.1084/jem.20110251

Cho, Y.S., S. Challa, D. Moquin, R. Genga, T.D. Ray, M. Guildford, and F.K.-M. Chan. 2009. Phosphorylation-driven assembly of the RIP1-RIP3

complex regulates programmed necrosis and virus-induced inflammation. *Cell*. 137:1112–1123. http://dx.doi.org/10.1016/j.cell.2009.05.037

Cook-Moreau, J.M., Y. El-Makhour Hojeij, G. Barrière, H.C. Rabinovitch-Chable, K.S. Faucher, F.G. Sturtz, and M.A. Rigaud. 2007. Expression of 5-lipoxygenase (5-LOX) in T lymphocytes. *Immunology*. 122:157–166. http://dx.doi.org/10.1111/j.1365-2567.2007.02621.x

D'Autréaux, B., and M.B. Toledano. 2007. ROS as signalling molecules: mechanisms that generate specificity in ROS homeostasis. *Nat. Rev. Mol. Cell Biol.* 8:813–824. http://dx.doi.org/10.1038/nrm2256

Declercq, W., T. Vanden Berghe, and P. Vandenabeele. 2009. RIP kinases at the crossroads of cell death and survival. *Cell*. 138:229–232. http://dx.doi.org/10.1016/j.cell.2009.07.006

Degterev, A., Z. Huang, M. Boyce, Y. Li, P. Jagtap, N. Mizushima, G.D. Cuny, T.J. Mitchison, M.A. Moskowitz, and J. Yuan. 2005. Chemical inhibitor of nonapoptotic cell death with therapeutic potential for ischemic brain injury. *Nat. Chem. Biol.* 1:112–119. http://dx.doi.org/10.1038/nchembio711

Devadas, S., L. Zaritskaya, S.G. Rhee, L. Oberley, and M.S. Williams. 2002. Discrete generation of superoxide and hydrogen peroxide by T cell receptor stimulation: selective regulation of mitogen-activated protein kinase activation and fas ligand expression. *J. Exp. Med.* 195:59–70. http://dx.doi.org/10.1084/jem.20010659

Dixon, S.J., K.M. Lemberg, M.R. Lamprecht, R. Skouta, E.M. Zaitsev, C.E. Gleason, D.N. Patel, A.J. Bauer, A.M. Cantley, W.S. Yang, et al. 2012. Ferroptosis: an iron-dependent form of nonapoptotic cell death. *Cell*. 149:1060–1072. http://dx.doi.org/10.1016/j.cell.2012.03.042

Fahey, R.C., and A.R. Sundquist. 1991. Evolution of glutathione metabolism. *Adv. Enzymol. Relat. Areas Mol. Biol.* 64:1–53.

Fan, J., H. Cai, S. Yang, L. Yan, and W. Tan. 2008. Comparison between the effects of normoxia and hypoxia on antioxidant enzymes and glutathione redox state in ex vivo culture of CD34(+) cells. *Comp. Biochem. Physiol.* 151:153–158. http://dx.doi.org/10.1016/j.cbpb.2008.06.008

Finkel, T. 2011. Signal transduction by reactive oxygen species. *J. Cell Biol.* 194:7–15. http://dx.doi.org/10.1083/jcb.201102095

Galkina, E., and K. Ley. 2009. Immune and inflammatory mechanisms of atherosclerosis (*). *Annu. Rev. Immunol.* 27:165–197. http://dx.doi.org/10.1146/annurev.immunol.021908.132620

Hameyer, D., A. Loonstra, L. Eshkind, S. Schmitt, C. Antunes, A. Groen, E. Bindels, J. Jonkers, P. Krimpenfort, R. Meuwissen, et al. 2007. Toxicity of ligand-dependent Cre recombinases and generation of a conditional Cre deleter mouse allowing mosaic recombination in peripheral tissues. *Physiol. Genomics*. 31:32–41. http://dx.doi.org/10.1152/physiolgenomics.00019.2007

Jackson, S.H., S. Devadas, J. Kwon, L.A. Pinto, and M.S. Williams. 2004. T cells express a phagocyte-type NADPH oxidase that is activated after T cell receptor stimulation. *Nat. Immunol.* 5:818–827. http://dx.doi.org/10.1038/ni1096

Lambert, A.J., H.M. Boysen, J.A. Buckingham, T. Yang, A. Podlutsky, S.N. Austad, T.H. Kunz, R. Buffenstein, and M.D. Brand. 2007. Low rates of hydrogen peroxide production by isolated heart mitochondria associate with long maximum lifespan in vertebrate homeotherms. *Aging Cell*. 6:607–618. http://dx.doi.org/10.1111/j.1474-9726.2007.00312.x

Lee, P.P., D.R. Fitzpatrick, C. Beard, H.K. Jessup, S. Lehar, K.W. Makar, M. Pérez-Melgosa, M.T. Sweetser, M.S. Schlissel, S. Nguyen, et al. 2001. A critical role for Dnmt1 and DNA methylation in T cell development, function, and survival. *Immunity*. 15:763–774. http://dx.doi.org/10.1016/S1074-7613(01)00227-8

Leto, T.L., and M. Geiszt. 2006. Role of Nox family NADPH oxidases in host defense. *Antioxid. Redox Signal.* 8:1549–1561. http://dx.doi.org/10.1089/ars.2006.8.1549

Levring, T.B., A.K. Hansen, B.L. Nielsen, M. Kongsbak, M.R. von Essen, A. Woetmann, N. Ødum, C.M. Bonefeld, and C. Geisler. 2012. Activated human $CD4^+$ T cells express transporters for both cysteine and cystine. *Sci. Rep.* 2:266. http://dx.doi.org/10.1038/srep00266

Lin, M.T., and M.F. Beal. 2006. Mitochondrial dysfunction and oxidative stress in neurodegenerative diseases. *Nature*. 443:787–795. http://dx.doi.org/10.1038/nature05292

Los, M., H. Schenk, K. Hexel, P.A. Baeuerle, W. Dröge, and K. Schulze-Osthoff. 1995. IL-2 gene expression and NF-kappa B activation through CD28 requires reactive oxygen production by 5-lipoxygenase. *EMBO J.* 14:3731–3740.

MacIver, N.J., R.D. Michalek, and J.C. Rathmell. 2013. Metabolic regulation of T lymphocytes. *Annu. Rev. Immunol.* 31:259–283. http://dx.doi.org/10.1146/annurev-immunol-032712-095956

Marnett, L.J. 2002. Oxy radicals, lipid peroxidation and DNA damage. *Toxicology*. 181-182:219–222. http://dx.doi.org/10.1016/S0300-483X(02)00448-1

Mougiakakos, D., C.C. Johansson, R. Jitschin, M. Böttcher, and R. Kiessling. 2011. Increased thioredoxin-1 production in human naturally occurring regulatory T cells confers enhanced tolerance to oxidative stress. *Blood*. 117:857–861. http://dx.doi.org/10.1182/blood-2010-09-307041

Navarro, F., P. Navas, J.R. Burgess, R.I. Bello, R. De Cabo, A. Arroyo, and J.M. Villalba. 1998. Vitamin E and selenium deficiency induces expression of the ubiquinone-dependent antioxidant system at the plasma membrane. *FASEB J.* 12:1665–1673.

Newton, K., X. Sun, and V.M. Dixit. 2004. Kinase RIP3 is dispensable for normal NF-kappa Bs, signaling by the B-cell and T-cell receptors, tumor necrosis factor receptor 1, and Toll-like receptors 2 and 4. *Mol. Cell. Biol.* 24:1464–1469. http://dx.doi.org/10.1128/MCB.24.4.1464-1469.2004

Niki, E., A. Kawakami, Y. Yamamoto, and Y. Kamiya. 1985. Oxidation of lipids. VIII. Synergistic inhibition of oxidation of phosphatidylcholine liposome in aqueous dispersion by vitamin E and vitamin C. *Bull. Chem. Soc. Jpn.* 58:1971–1975. http://dx.doi.org/10.1246/bcsj.58.1971

Pearce, E.L., and E.J. Pearce. 2013. Metabolic pathways in immune cell activation and quiescence. *Immunity*. 38:633–643. http://dx.doi.org/10.1016/j.immuni.2013.04.005

Pircher, H., K. Bürki, R. Lang, H. Hengartner, and R.M. Zinkernagel. 1989. Tolerance induction in double specific T-cell receptor transgenic mice varies with antigen. *Nature*. 342:559–561. http://dx.doi.org/10.1038/342559a0

Planz, O., S. Ehl, E. Furrer, E. Horvath, M.A. Bründler, H. Hengartner, and R.M. Zinkernagel. 1997. A critical role for neutralizing-antibody-producing B cells, CD4(+) T cells, and interferons in persistent and acute infections of mice with lymphocytic choriomeningitis virus: implications for adoptive immunotherapy of virus carriers. *Proc. Natl. Acad. Sci. USA*. 94:6874–6879. http://dx.doi.org/10.1073/pnas.94.13.6874

Ray, P.D., B.-W. Huang, and Y. Tsuji. 2012. Reactive oxygen species (ROS) homeostasis and redox regulation in cellular signaling. *Cell. Signal.* 24:981–990. http://dx.doi.org/10.1016/j.cellsig.2012.01.008

Rooke, R., C. Waltzinger, C. Benoist, and D. Mathis. 1997. Targeted complementation of MHC class II deficiency by intrathymic delivery of recombinant adenoviruses. *Immunity*. 7:123–134. http://dx.doi.org/10.1016/S1074-7613(00)80515-4

Sattler, W., M. Maiorino, and R. Stocker. 1994. Reduction of HDL- and LDL-associated cholesterylester and phospholipid hydroperoxides by phospholipid hydroperoxide glutathione peroxidase and Ebselen (PZ 51). *Arch. Biochem. Biophys.* 309:214–221. http://dx.doi.org/10.1006/abbi.1994.1105

Schneider, M., M. Wortmann, P.K. Mandal, W. Arpornchayanon, K. Jannasch, F. Alves, S. Strieth, M. Conrad, and H. Beck. 2010. Absence of glutathione peroxidase 4 affects tumor angiogenesis through increased 12/15-lipoxygenase activity. *Neoplasia*. 12:254–263.

Seiler, A., M. Schneider, H. Förster, S. Roth, E.K. Wirth, C. Culmsee, N. Plesnila, E. Kremmer, O. Rådmark, W. Wurst, et al. 2008. Glutathione peroxidase 4 senses and translates oxidative stress into 12/15-lipoxygenase dependent- and AIF-mediated cell death. *Cell Metab.* 8:237–248. http://dx.doi.org/10.1016/j.cmet.2008.07.005

Selin, L.K., M.Y. Lin, K.A. Kraemer, D.M. Pardoll, J.P. Schneck, S.M. Varga, P.A. Santolucito, A.K. Pinto, and R.M. Welsh. 1999. Attrition of T cell memory: selective loss of LCMV epitope-specific memory CD8 T cells following infections with heterologous viruses. *Immunity*. 11:733–742. http://dx.doi.org/10.1016/S1074-7613(00)80147-8

Sena, L.A., S. Li, A. Jairaman, M. Prakriya, T. Ezponda, D.A. Hildeman, C.-R. Wang, P.T. Schumacker, J.D. Licht, H. Perlman, et al. 2013. Mitochondria are required for antigen-specific T cell activation through reactive oxygen species signaling. *Immunity*. 38:225–236. http://dx.doi.org/10.1016/j.immuni.2012.10.020

Smith-Garvin, J.E., G.A. Koretzky, and M.S. Jordan. 2009. T cell activation. *Annu. Rev. Immunol.* 27:591–619. http://dx.doi.org/10.1146/annurev.immunol.021908.132706

Sun, D., and C.D. Funk. 1996. Disruption of 12/15-lipoxygenase expression in peritoneal macrophages. Enhanced utilization of the 5-lipoxygenase pathway and diminished oxidation of low density lipoprotein. *J. Biol. Chem.* 271:24055–24062. http://dx.doi.org/10.1074/jbc.271.39.24055

Tanchot, C., F.A. Lemonnier, B. Pérarnau, A.A. Freitas, and B. Rocha. 1997. Differential requirements for survival and proliferation of CD8 naïve or memory T cells. *Science.* 276:2057–2062. http://dx.doi.org/10.1126/science.276.5321.2057

Tappel, A.L. 1972. Vitamin E and free radical peroxidation of lipids. *Ann. N. Y. Acad. Sci.* 203:12–28. http://dx.doi.org/10.1111/j.1749-6632.1972.tb27851.x

Thomas, J.P., M. Maiorino, F. Ursini, and A.W. Girotti. 1990. Protective action of phospholipid hydroperoxide glutathione peroxidase against membrane-damaging lipid peroxidation. In situ reduction of phospholipid and cholesterol hydroperoxides. *J. Biol. Chem.* 265:454–461.

Toyokuni, S., K. Okamoto, J. Yodoi, and H. Hiai. 1995. Persistent oxidative stress in cancer. *FEBS Lett.* 358:1–3. http://dx.doi.org/10.1016/0014-5793(94)01368-B

van der Windt, G.J.W., B. Everts, C.-H. Chang, J.D. Curtis, T.C. Freitas, E. Amiel, E.J. Pearce, and E.L. Pearce. 2012. Mitochondrial respiratory capacity is a critical regulator of CD8+ T cell memory development. *Immunity.* 36:68–78. http://dx.doi.org/10.1016/j.immuni.2011.12.007

Walsh, C.M., B.G. Wen, A.M. Chinnaiyan, K. O'Rourke, V.M. Dixit, and S.M. Hedrick. 1998. A role for FADD in T cell activation and development. *Immunity.* 8:439–449. http://dx.doi.org/10.1016/S1074-7613(00)80549-X

Wang, R., and D.R. Green. 2012. Metabolic checkpoints in activated T cells. *Nat. Immunol.* 13:907–915. http://dx.doi.org/10.1038/ni.2386

Winterbourn, C.C. 2008. Reconciling the chemistry and biology of reactive oxygen species. *Nat. Chem. Biol.* 4:278–286. http://dx.doi.org/10.1038/nchembio.85

Yagoda, N., M. von Rechenberg, E. Zaganjor, A.J. Bauer, W.S. Yang, D.J. Fridman, A.J. Wolpaw, I. Smukste, J.M. Peltier, J.J. Boniface, et al. 2007. RAS-RAF-MEK-dependent oxidative cell death involving voltage-dependent anion channels. *Nature.* 447:864–868. http://dx.doi.org/10.1038/nature05859

Yang, W.S., R. SriRamaratnam, M.E. Welsch, K. Shimada, R. Skouta, V.S. Viswanathan, J.H. Cheah, P.A. Clemons, A.F. Shamji, C.B. Clish, et al. 2014. Regulation of ferroptotic cancer cell death by GPX4. *Cell.* 156:317–331. http://dx.doi.org/10.1016/j.cell.2013.12.010

Yant, L.J., Q. Ran, L. Rao, H. Van Remmen, T. Shibatani, J.G. Belter, L. Motta, A. Richardson, and T.A. Prolla. 2003. The selenoprotein GPX4 is essential for mouse development and protects from radiation and oxidative damage insults. *Free Radic. Biol. Med.* 34:496–502. http://dx.doi.org/10.1016/S0891-5849(02)01360-6

Yi, J.S., B.C. Holbrook, R.D. Michalek, N.G. Laniewski, and J.M. Grayson. 2006. Electron transport complex I is required for CD8+ T cell function. *J. Immunol.* 177:852–862. http://dx.doi.org/10.4049/jimmunol.177.2.852